

Effect of size and distribution of titanium carbide on microstructure and mechanical properties of Ti-25V-15Cr-2Al-0.2C-0.2Si alloy^①

LEI Li-ming(雷力明)¹, HUANG Xu(黄旭)¹, WANG Bao(王宝)¹,
ZHAO Hong-xia(赵红霞)¹, CAO Chun-xiao(曹春晓)¹, D. Rugg², W. Voice²
(1. Laboratory of Titanium Alloys, Beijing Institute of Aeronautical Materials,
Beijing 100095, China;
2. Rolls-Royce Plc, P. O. Box 31, Derby DE24 8BJ, U. K.)

Abstract: The effect of size and distribution of titanium carbide on the microstructure and mechanical properties of non-burning β titanium alloy Ti-25V-15Cr-2Al-0.2C-0.2Si (mass fraction, %) was investigated. The microstructure of the heat-treated and exposed alloy was studied using optical microscopy (OM), scanning electron microscopy (SEM) and transmission electron microscopy (TEM). It is found that carbides with finer size and more uniform distribution can suppress the formation of α precipitates more effectively, and can especially decrease the amount of grain boundary α precipitates after long-term exposure at 540 °C (the expected application temperature). Thus, significant improvement in thermal stability can be achieved by refining carbide particles in the matrix of the alloy.

Key words: non-burning; titanium alloy; carbide; mechanical properties

CLC number: TG 146.23

Document code: A

1 INTRODUCTION

In the early 1990s, Pratt & Whitney in the USA developed a non-burning alloy based on Ti-35V-15Cr, designated Alloy C^[1, 2]. The production cost of this alloy is very high because of a large amount of expensive vanadium addition. In recent work undertaken jointly by the IRC and Rolls-Royce in UK^[3-6], a low-cost non-burning alloy has been developed with nominal composition Ti-25V-15Cr-2Al-0.2C. The effect of carbon additions on microstructure and mechanical properties of non-burning titanium alloy Ti-25V-15Cr-2Al has been studied by Li et al^[5, 6]. It was found that carbon additions significantly improved the ductility of the alloy. The α precipitation was reduced through gettering of oxygen by carbides, thus the stability of the alloy was improved. 0.2% carbon was considered to be the optimum content added to the Ti-25V-15Cr-2Al alloy^[7]. However, after long-term exposure a large number of α phases still precipitate at expected application temperatures (although much less than those in alloys without carbon additions), which can degrade the ductility of the alloy drastically^[8-11]. In the previous study^[10], a particular heat treatment process was introduced to improve the ductility of the alloy after exposure. The objective of the present work is to study the effect of size and distribution of carbide on microstructure

and mechanical properties of Ti-25V-15Cr-2Al-0.2C-0.2Si alloy. We have found that it is possible to significantly improve the ductility of the alloy by refining carbide particles. It should also be noted that 0.2% Si addition was used to improve the creep properties of the alloy, whose effect on the microstructure and properties of the alloy will be discussed in other articles.

2 EXPERIMENTAL

After mixing and compacting raw materials of Ti-25V-15Cr-2Al-0.2C-0.2Si alloy, a 15 kg ingot was produced by vacuum arc remelting (VAR). The chemical composition of the ingot is listed in Table 1.

Table 1 Chemical composition of alloy (mass fraction, %)

Ti	V	Cr	Al	C
Balance	25.4	14.7	1.95	0.21
Si	O	N	H	
0.2	0.078	0.006	< 0.002	

The ingot was forged and finally hot-rolled into bars with 18.5 mm diameter, some (sample S1) of which underwent larger deforming compared

① **Foundation item:** Project(2000 - 2005) supported by Beijing Institute of Aeronautical Materials in China and Rolls-Royce Plc in UK

Received date: 2004 - 10 - 20; **Accepted date:** 2005 - 01 - 14

Correspondence: LEI Li-ming, PhD; Tel: + 86-10-62496627; E-mail: liming.lei@biam.ac.cn

with the others (sample S2) so that carbides with different sizes and distribution were obtained. All of the samples were solution-treated at 1050 °C for 30 min and aged at 700 °C for 4 h (named condition 1 in this paper) to obtain a fully recrystallized and stabilized microstructure. In order to investigate the thermal stability of the alloy, the heat-treated samples were exposed for 100 h at 540 °C (named condition 2).

All samples were cut, polished and etched for optical microscopy (OM) and scanning electron microscopy (SEM) study. The etchant consisted of 5% HF, 10% HNO₃ and 85% H₂O (volume fraction). Thin foils for transmission electron microscopy (TEM) were prepared by a twin-jet electropolishing technique, using an electrolyte composed of 6% perchloric acid, 34% n-butanol and 60% methanol at about 40 V and –30 °C. TEM observations were carried out on a JEOL-200CX transmission electron microscope operated at 200 kV. Fracture surfaces were observed using a JSM-5600LV scanning electron microscope filled with LINK ISIS300 EDX analytical systems operated at 20 kV.

3 RESULTS

3.1 As-cast and as-forged microstructures

Fig. 1(a) shows the microstructure of as-cast samples of the alloy. It can be seen that titanium carbides formed by a eutectic reaction in terms of the Ti-C binary diagram^[12] are presented as long rods in the β matrix. Primary large β grains are such that grain boundaries can not be observed in the as-cast microstructure.

Fig. 1(b) shows the microstructure of as-forged samples. The as-cast microstructure of the alloy is broken down and some fine β grains are obtained. Moreover, it can also be clearly seen that primary long-rod shape carbides fracture into short-rod or globular particles, which are homogeneously distributed in grains and on grain boundaries. Obviously, the direct impact of fine carbide particles on the microstructure of the alloy is to refine the as-forged microstructure.

Fig. 2 shows the morphology and corresponding SAD pattern of a carbide particle. As reported by Li et al^[6], some superlattice spots can be seen in the [011] pole SAD pattern (see inset in Fig. 2), indicating that the carbides have an ordering structure. It was found that the intensity of these spots decreased and eventually disappeared with the time of exposure to the electron beam.

3.2 Effect of size and distribution of carbide on heat treatment and exposure microstructure of samples

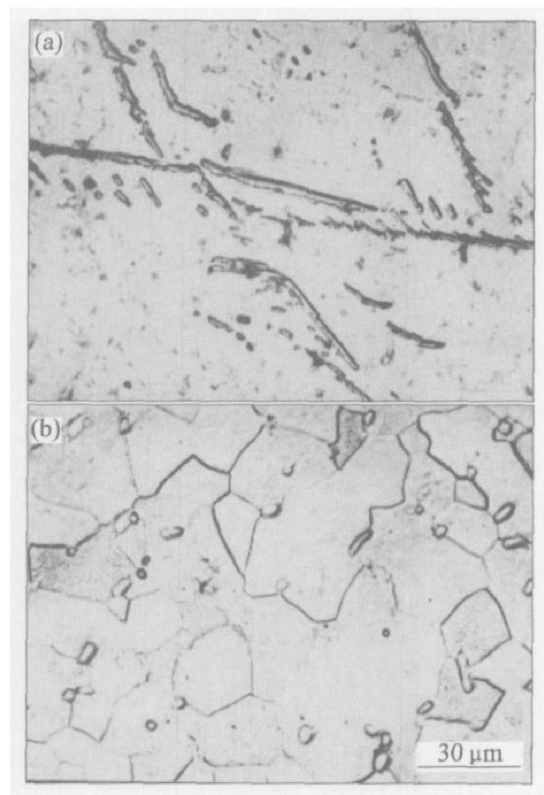


Fig. 1 Optical microstructures of Ti-25V-15Cr-2Al-0.2C-0.2Si alloy
(a) —As-cast; (b) —As-forged

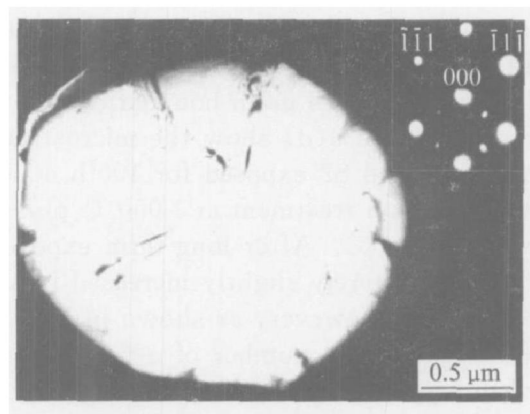


Fig. 2 TEM micrograph of carbide precipitation
(The inset is a SAD pattern taken from [011] pole of carbide)

SEM secondary electron micrographs in Figs. 3(a) and (b) show the microstructures of samples S1 and S2 (cf. section 2) aged at 700 °C for 4 h following solution treatment at 1050 °C for 30 min. It can be clearly observed that the microstructure of sample S1 (Fig. 3(a)) has much finer β grains (about 50 μ m) and carbides (about 2 μ m) as compared with that of sample S2 in which the average sizes of β grains and carbides are about 90 μ m and 4 μ m, respectively (Fig. 3(b)). Moreover, carbide particles are more uniformly distributed both in grains and on grain boundaries in sample S1 compared with sample S2. Except for the difference in the average sizes of carbide particles and β grains, it is especially interesting to note that only a little

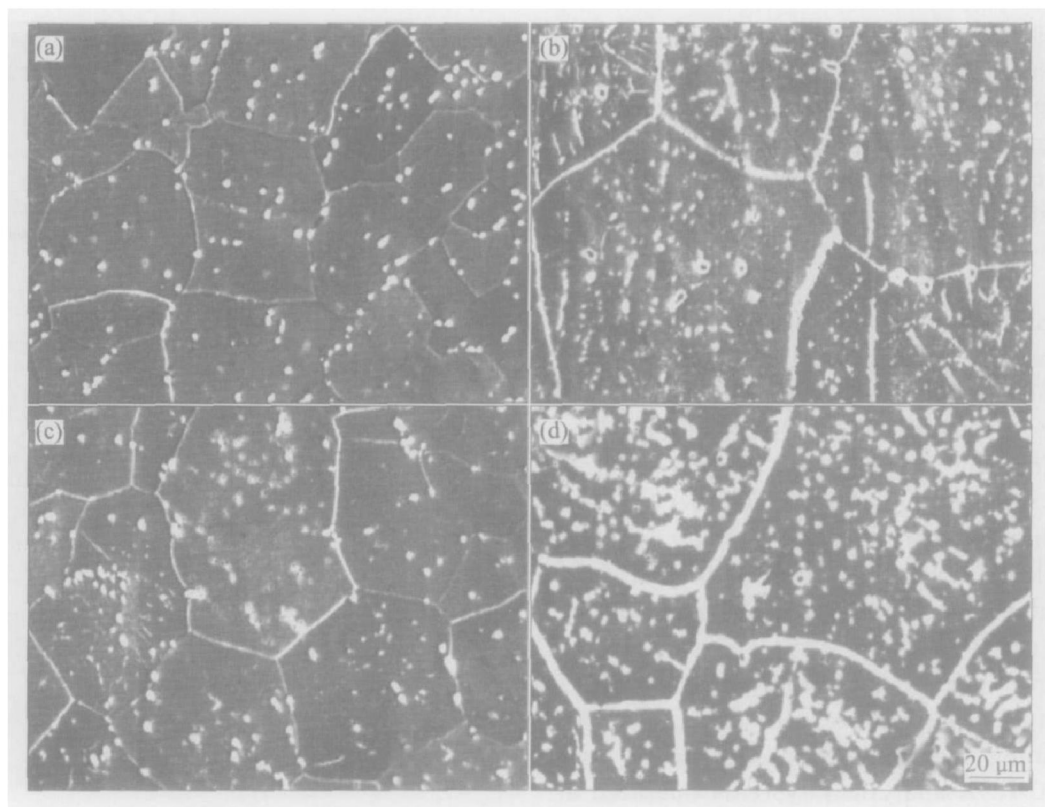


Fig. 3 SEM microstructures of Ti-25V-15Cr-2Al-0.2C-0.2Si alloy under different conditions
 (a) —Sample S1, condition 1; (b) —Sample S2, condition 1;
 (c) —Sample S1, condition 2, (d) —Sample S2, condition 2

α precipitation is seen in sample S1, whereas in sample S2 higher level of α precipitation is produced in grains and on grain boundaries.

Figs. 3(c) and 3(d) show the microstructures of samples S1 and S2 exposed for 100 h at 540 °C following solution treatment at 1 050 °C plus aging treatment at 700 °C. After long-term exposure, α precipitation is merely slightly increased in sample S1 (Fig. 3(c)). However, as shown in Fig. 3(d), a markedly increased number of α precipitates are formed in exposed sample S2 when compared with the sample S2 without exposure (Fig. 3(b)). TEM micrographs in Figs. 4(a) and (b) show the morphologies of grain boundary α (GB α) precipitates in samples S1 and S2 exposed for 100 h at 540 °C. The number of GB α precipitates in sample S2 is greatly larger than that in sample S1 so that a continuous α film is formed (Fig. 4(b)).

3.3 Tensile properties

The results of room temperature tensile properties of samples S1 and S2 are listed in Table 2. It can be seen from Table 2 that sample S1 has significantly higher ductility than sample S2 under the same conditions though they are not as strong. The elongation of sample S1 under condition 1 is 4 times as large as that of sample S2 under the same condition. It is noteworthy that after exposure at 540 °C for 100 h the ductility of sample S2 seems to be entirely lost whereas that of sample S1 is only

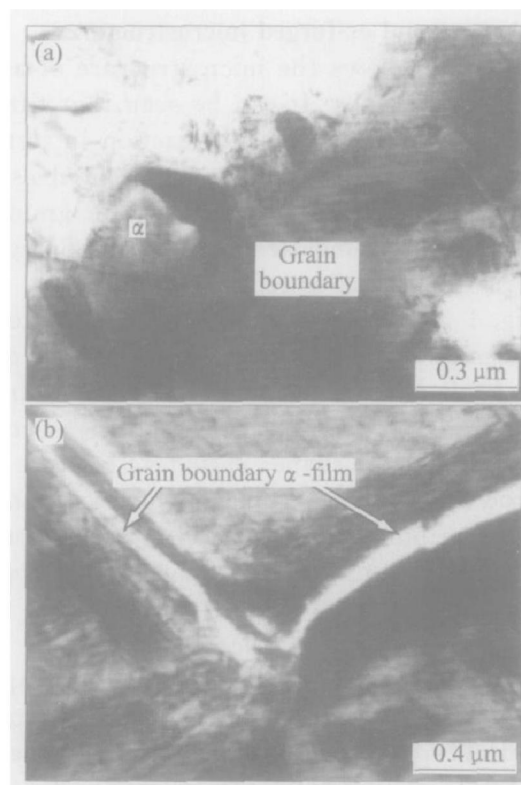


Fig. 4 TEM micrographs of GB α precipitates in Ti-25V-15Cr-2Al-0.2C-0.2Si alloy
 (a) —Sample S1; (b) —Sample S2

slightly decreased.

As indicated by previous work^[7, 13, 14], the loss of ductility of Ti-25V-15Cr- x system alloys is closely related to the presence of α precipitation.

Table 2 Tensile properties of samples S1 and S2

Sample	Heat treatment	σ_b /MPa	$\sigma_{b,2}$ /MPa	δ /%	ψ /%
S1	Condition 1	1 015	997	20	44
	Condition 2	1 005	990	17	33
S2	Condition 1	1 079	1 048	5	14
	Condition 2	1 054	—	—	—

Condition 1 —1 050 °C, 0.5h, air cooling+ 700 °C, 4 h, air cooling; Condition 2 —Condition 1 + 540 °C, 100 h, air cooling

Since the formation of α precipitates is greatly suppressed in sample S1, the significant improvement in ductility is obtained. Furthermore, the refined β grains also contribute to the enhancement in the ductility of sample S1. In contrast, the ductility of sample S2 is very low due to the occurrence of the higher level of α precipitation, especially the continuous GB α film formed after exposure leads to the exhausted ductility.

3.4 Fractograph observation

Fig. 5 shows the tensile fracture surfaces of samples S1 and S2 at room temperature. In Fig. 5 (a), the ductile dimples can be seen throughout the fracture surface of sample S1 under condition 1, indicating a micro-void coalescence mode. However, the fracture surface of sample S2 under condition 1 mainly fails by intergranular cracking (Fig. 5(b)). As shown in Figs. 5(c) and (d), after

long-term exposure sample S1 fractures by a mixture of transgranular and ductile intergranular modes, whereas sample S2 shows typical brittle intergranular fracture.

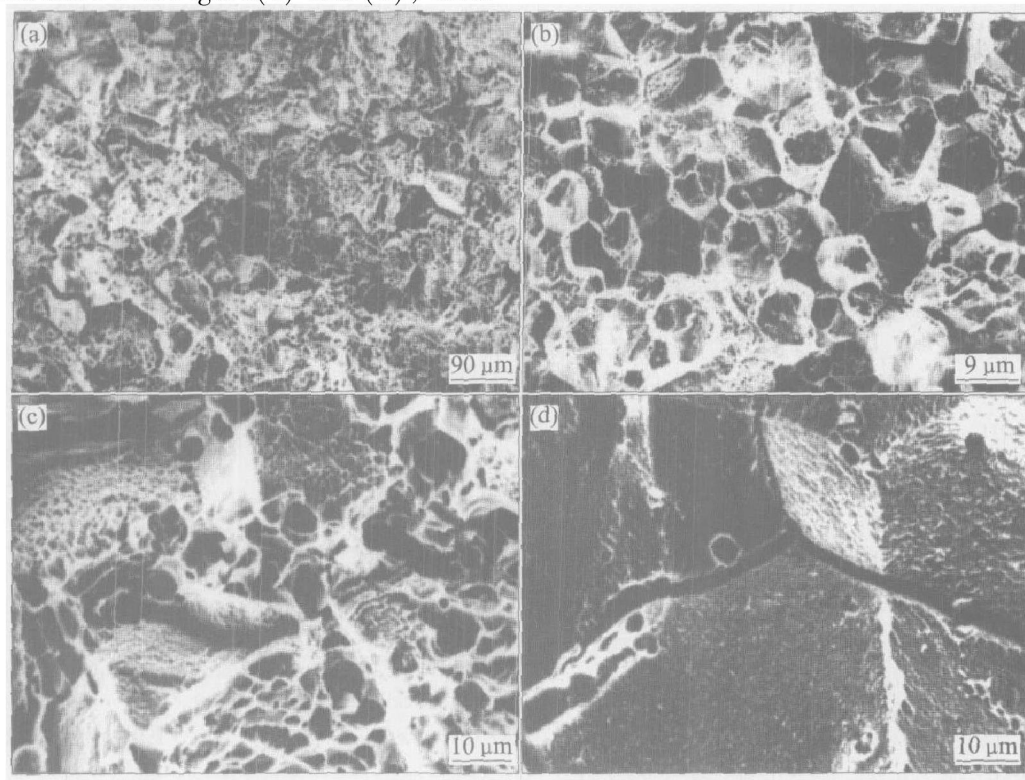
The results of fractograph examination are consistent with the changes in the ductility listed in Table 2. It is obvious that the existence of excessive GB α mainly leads to the intergranular fracture of sample S2, due to facilitating crack propagation.

4 DISCUSSION

It has been confirmed that carbides in Ti-V-Cr system alloys can provide a stable sink for interstitial oxygen, a strong α stabilizing element, in the β matrix^[6, 15]. Carbon additions can significantly reduce α precipitation, thus the ductility of the alloys are improved. Since the number of carbides mainly depends on the carbon content added to the experimental alloy, the volume fraction of carbide particles remains almost constant (approximately 4%). The mean planar particle spacing l reduces with a decrease in average particle size according to the formula^[16]:

$$l = r \sqrt{\frac{2\pi}{3\varphi}}$$

where φ is the volume fraction of particles, r is the average particle radius. This means that the diffusion distance of interstitial oxygen toward carbides is significantly decreased as well, thus leading to that interstitial oxygen in the matrix can be

**Fig. 5** SEM fractographs of room temperature tensile surfaces of samples S1 and S2

(a) —Sample S1, condition 1; (b) —Sample S2, condition 1;
(c) —Sample S1, condition 2; (d) —Sample S2, condition 2

more sufficiently absorbed by carbides. This will further suppress the formation of α precipitation in grains and on grain boundaries.

Besides the possible reason mentioned above, the very low level of GB α precipitation in sample S1 is also believed to be associated with other two factors. As mentioned earlier, a direct effect of fine carbide is to refine the as-forged and heat-treated microstructure of the alloy. The finer and more uniformly distributed the carbide particles are, the larger the effect is. The decrease in β grain size enhances the grain boundary area available for α precipitates, thereby less α on each boundary. On the other hand, the markedly refined carbide particles in sample S1 result in higher density of carbide/ β matrix interfaces, a few of which possibly act as α nucleation sites (see Fig. 6), thus reducing the tendency of α precipitating preferentially on β grain boundaries.

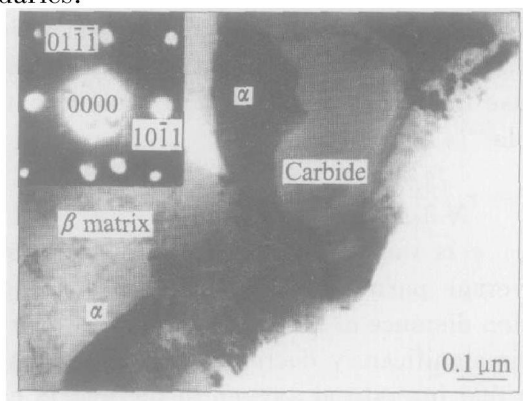


Fig. 6 TEM morphology of α precipitation on β carbide interface
(The inset is a SAD pattern taken from $[\bar{1}01]$ pole of α phase)

5 CONCLUSIONS

The effect of size and distribution of titanium carbide on the microstructure and mechanical properties of Ti-25V-15Cr-2Al-0.2C-0.2Si non-burning β titanium alloy was investigated. It was found that finer and more uniformly distributed carbide particles can more effectively suppress the formation of α precipitates detrimental to the ductility of the alloy, besides playing a direct role in refining the as-forged and heat-treated microstructure of the alloy. Thus, the significant improvement in the ductility can be achieved by refining the primary carbide particles formed mainly from the melt.

REFERENCES

[1] Giary K. High-strength titanium resistant ignition[J]. *Adv Mater Proc*, 1993, 9: 7-10.
[2] Seagle S R. The state of the USA titanium industry in 1995[J]. *Mater Sci Eng*, 1996, A213: 1-7.
[3] Li Y G, Blenkinsop P A, Loretto M H, et al. Effect

of aluminium on ordering of highly stabilized β Ti-V-Cr alloys[J]. *Materials Science and Technology*, 1998, 14 (8): 732-737.

- [4] Li Y G, Blenkinsop P A, Loretto M H, et al. Effect of aluminum on deformation structure of highly stabilized β Ti-V-Cr alloys[J]. *Materials Science and Technology*, 1999, 15 (2): 151-155.
[5] Li Y G, Blenkinsop P A, Loretto M H, et al. Effect of carbon on α precipitation and tensile properties of β TiVCrAl alloys[A]. Gorynin I V, Ushkov S S. *Proceedings of the 9th World Conference on Titanium[C]*. Moscow: Central Research Institute of Structural Materials (CRISM) "Prometey", 1999. 141-148.
[6] Li Y G, Blenkinsop P A, Loretto M H, et al. Effect of carbon and oxygen on microstructure and mechanical properties of Ti-25V-15Cr-2Al alloy[J]. *Acta Mater*, 1999, 47 (10): 2889-2905.
[7] Li Y G, Loretto M H, Rugg D, et al. Effect of heat treatment and exposure on microstructure and mechanical properties of Ti-25V-15Cr-2Al-0.2C alloy[J]. *Acta Mater*, 2001, 49 (11): 3011-3017.
[8] LEI Lǐmíng, HUANG Xu, SUN Fúshèng, et al. Microstructure, tensile properties and deformation mechanisms of Ti-25V-15Cr-2Al-0.2C alloy[J]. *The Chinese Journal of Nonferrous Metals*, 2003, 13(4): 939-943. (in Chinese)
[9] LEI Lǐmíng, HUANG Xu, SUN Fúshèng, et al. Effect of thermal exposure on microstructure of Ti-25V-15Cr-2Al-0.2C alloy[J]. *Chinese Journal of Rare Metals*, 2003, 27(1): 207-209. (in Chinese)
[10] LEI Lǐmíng, HUANG Xu, SUN Fúshèng, et al. Heat treatment process for improving the ductility of Ti-25V-15Cr-2Al-0.2C [J]. *Trans Nonferrous Met Soc China*, 2003, 13(5): 1175-1180.
[11] HUANG Xu, LEI Lǐmíng, SUN Fúshèng et al. Study of microstructure and phase constituent of Ti-25V-15Cr-2Al-0.2C alloy[J]. *Rare Metal Materials and Engineering*, 2004, 33(2): 218-221. (in Chinese)
[12] Baker H. Alloy Phase Diagrams: Binary Alloy Phase Diagrams[M]. Ohio: ASM International, 1992. 2-114.
[13] Li Y G, Blenkinsop P A, Loretto M H, et al. Structure and stability of precipitates in 500 °C exposed Ti-25V-15Cr-xAl alloys[J]. *Acta Mater*, 1998, 46(16): 5777-5794.
[14] LEI Lǐmíng, HUANG Xu, SUN Fúshèng, et al. Effects of second phases on tensile fracture behavior of Ti-25V-15Cr-2Al-0.2C-x alloys[J]. *Chinese Journal of Rare Metals*, 2004, 28(1): 47-49. (in Chinese)
[15] Hansen J O, Novotnak D, Welter M F, et al. Properties and processing of a high strength beta titanium alloy[A]. *Proceedings of the 8th World Conference on Titanium[C]*. London: The Institute of Materials, 1996. 675-682.
[16] FENG Duan. Metal Physics (Vol. 3)[M]. Beijing: Science Press, 1999. 420. (in Chinese)

(Edited by YUAN Sǎi-qian)